Volume 9
Number 46
14 December 2021
Pages 16327–16790

Journal of Materials Chemistry C

Materials for optical, magnetic and electronic devices

rsc.li/materials-c

ISSN 2050-7526

ROYAL SOCIETY OF CHEMISTRY

PAPER

Mi Jung Lee *et al.*

Knitted strain sensor with carbon fiber and aluminum-coated yarn, for wearable electronics

Journal of Materials Chemistry C

ROYAL SOCIETY OF CHEMISTRY

PAPER

View Article Online
View Journal | View Issue

Cite this: J. Mater. Chem. C, 2021, 9, 16440

Knitted strain sensor with carbon fiber and aluminum-coated yarn, for wearable electronics†

Junhyeok Jang,‡[a] Suji Kim,‡[a] Kangmin Lee,[a] Seungjun Park,[a] Geum-Yong Park,[b] Byoung-Joon Kim,[b] Junghun Oh[c] and Mi Jung Lee *[a]

Received 24th April 2021,
Accepted 27th September 2021

DOI: 10.1039/d1tc01899j

rsc.li/materials-c

A knitted textile-type strain sensor with resistive random access memory (RRAM) characteristics is developed. This study focuses on the change in resistance at the contact between carbon and aluminum fibers along the strain to develop a strain sensor that can be used in smart clothing. Unlike conventional textile sensors that use only one type of conducting yarn, this study proposes a new configuration that uses two different materials to obtain a large change in resistance value. The all-in-one yarn, comprising carbon fibers, aluminum-coated yarns, and normal yarns, was used to construct sensor devices by knitting. In this knitted textile, the resistance switching characteristics of the RRAM between aluminum and carbon were observed as confirmed in previous studies for flat devices and woven textiles. Along the strain applied to the knitted fabric sensor, the change in the resistance along the stretching was detected and verified through a physical mechanism of the change in the contact area. The sensitivity of the developed knitted strain sensor is more than 10 times higher than previously demonstrated textile strain sensors. Also, cyclic testing of the sensor between the stretched and the recovered state on a machine and on a knee was demonstrated to prove that it can be used as a motion sensor by applying it to the joint part of clothing. In addition, there are advantages of low-cost and large-scale production that are possible since this yarn can be used in existing fabric production industries.

1. Introduction

E-textiles are a representative technology that are applicable to smart clothing, which is a fabric with embedded functional electronic devices.[1–3] In the early stages, they were achieved by attaching various kinds of electronic device onto clothes. Recently, research has been active on inherently textile-like devices such as fiber transistors, piezoelectric temperature sensors, and fiber displays based on yarn-type conductive fibers.[4,5] Studies on e-textiles under extreme conditions, such as mechanical bending, folding, stretching, and washing, have also been very active for extending the applications of e-textiles.[6–9]

Through our previous research on e-textiles using conducting yarns, we have succeeded in developing the textile-type RRAM (resistive random access memory) that is composed of a yarn coated with aluminum using a solution process, and a carbon fiber yarn through a typical weaving method that is the same as is used for normal yarns.[10]

In this study, we focus on the resistance-changing characteristics at the contact points between yarns as well as with the stretching of knitted textiles, and a strain sensor was developed that can be used in smart clothing. The aluminum-coated yarn with a thin native oxide layer and the carbon fiber yarn allowed the goal of fabricating strain sensors through large resistance-changing characteristics upon stretching to be achieved. The sensor was made in the form of a knitted textile that comprises aluminum-coated yarn, carbon fiber yarn, and normal yarn. The knitted textile sensors developed here use two materials that show different mechanisms from previously reported textile sensors and demonstrate a great advantage in sensitivity.

Since aluminum is a popular conducting material with a high electrical conductivity and low cost,[11] the chemical process of making aluminum nanoparticles is broadly achieved through the decomposition of the aluminum precursor (AlH_3) into aluminum and H_2[12–17] (see the Experimental section). Then the oxidation of aluminum occurs immediately after the formation of aluminum nanoparticles on the surface of the yarn.[12] The typical

[a] School of Advanced Materials Engineering, Kookmin University, Seoul, 02707, South Korea. E-mail: mijung@kookmin.ac.kr
[b] Department of Advanced Materials Engineering, Korea Polytechnic University, D-405, 237 Sangidaehar-ro, Siheung-si, Gyeonggi-do, 15073, Korea. E-mail: bjkim@kpu.ac.kr; Fax: +82-31-8041-0599; Tel: +82-31-8041-0593
[c] Department of Electronic Engineering, Kookmin University, Seoul, 02707, South Korea

† Electronic supplementary information (ESI) available. See DOI: 10.1039/d1tc01899j

‡ These authors contributed equally to this work.

thickness of the native aluminum oxide layer on the coated aluminum is ~5 nm.[18]

In this knitted textile, the resistive switching characteristics were shown as confirmed in a previous study.[10] Then, the samples were stretched in both the horizontal and vertical directions to demonstrate a change of the resistance along the stretch. The resistance between the aluminum yarn and the carbon yarn was decreased when stretched, and was restored to the ratio before stretching when the textile was recovered. It was also proved that this characteristic is maintained when stretching and recovery are repeated along the cyclic test. We expect that the textile-type strain sensor developed in this study can be used as a strain sensor/motion sensor by applying it to the joint part of clothing.

2. Materials and methods

2.1 Precursor solution for the preparation of highly conductive aluminum-coated yarn

The aluminum precursor solution has to be prepared to make highly conductive aluminum-coated yarn through the solution process. For the preparation of the aluminum precursor solution, a chemical reaction of aluminum chloride ($AlCl_3$) with lithium aluminum hydride ($LiAlH_4$, LAH) was used. Anhydrous dibutyl ether ($C_8H_{18}O$) was used in the reaction as a solvent. $AlCl_3$, LAH, and $C_8H_{18}O$ were purchased from Sigma-Aldrich Chemicals and used without any extra treatment. After $AlCl_3$ and LAH powders were added to the solvent, the mixed solution was heated at (75 °C) with stirring for more than 2 hours.[12–14,16] The gray slurry remaining after mixing was filtered with a PVDF filter (0.45 μm) to obtain a clear aluminum precursor solution.

2.2 Dipping process for the preparation of highly conductive aluminum-coated yarn

A preheated spun rayon yarn (75%) with catalytic treatment was coated with the aluminum precursor solution[19] by dipping and drying overnight at room temperature. To ensure high conductivity and uniformity of the coating layer, all of these processes were carried out under a nitrogen atmosphere to prevent the formation of aluminum hydroxide ($Al(OH)_3$), aluminum nitride (AlN), or aluminum oxide (Al_2O_3).

2.3 Fabrication and measurement of the textile-type RRAM for textile strain sensor

The textile-type RRAM (resistive RAM) was knitted using a hand-knitting machine. The basic knitted fabric with cotton yarn has the built-in textile RRAM that consists of aluminum-coated yarn and 1 k carbon fiber yarn (*i.e.*, one thread of 1000 fibers).[20–22] The device was stretched at intervals (of 5 mm) and then released to be recycled. The stretching test was performed by pulling both ends of the device in horizontal and vertical directions, respectively. The stretching test was conducted using a commercial mechanical test machine (CKSI, Korea) and an electrical measurement system (KEITHLEY 2400). The variation of the resistance was measured using an MS TECH probe station with a KEITHLEY SCS 4200 system. To verify the static and dynamic reliability of the textile-type resistance strain sensor, the stretching test and measurement of the output voltage change were performed simultaneously. A simple voltage divider circuit (Arduino) was designed to measure the voltage output during bending and recovery of the sample. The Arduino circuits and devices were connected using conductive thread or special sample-fixing pins for measuring the electrical properties, and changes in the output voltage due to stretching and recovery were observed.

3. Results and discussion

The schematic diagram of the device, the basic current and voltage properties of resistive switching, and the endurance properties of the aluminum–carbon RRAM are shown in Fig. 1. The RRAM structure in Fig. 1a shows a single cross-contact device between the aluminum film and the carbon fiber when they were simply placed across each other by physical contact. Native aluminum oxide is formed on top of the aluminum film, which plays a critical role in resistive switching, and which was proved in previous work.[10] The current–voltage characteristics of a single contact point show the typical bipolar resistive switching properties[23–25] of a conventional metal–insulator–metal (MIM) RRAM structure,[26–29] as shown in Fig. 1b, even though the device has a metal–metal (MM) structure,[10] and resistive switching between a high resistance state (HRS) and a low resistance state (LRS) is observed with an on/off resistance

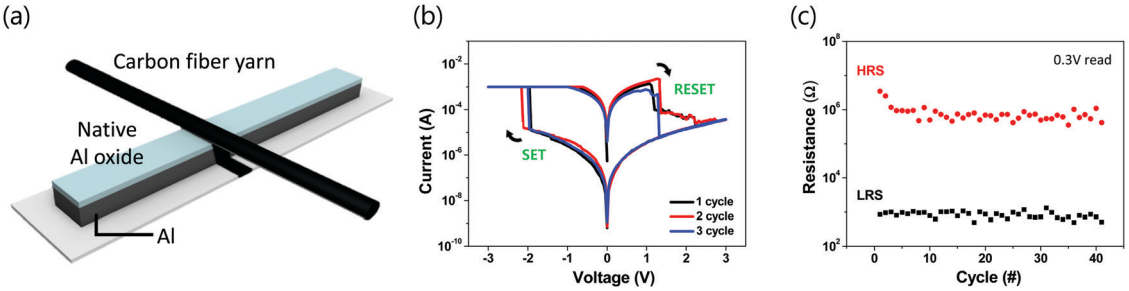

Fig. 1 Structure and characteristics of the film-type aluminum–carbon RRAM: (a) schematic structure of the RRAM with a carbon fiber yarn and an aluminum film with an aluminum oxide layer, (b) *I*–*V* characteristics of the aluminum–carbon RRAM, and (c) endurance properties over set/reset operation cycles.

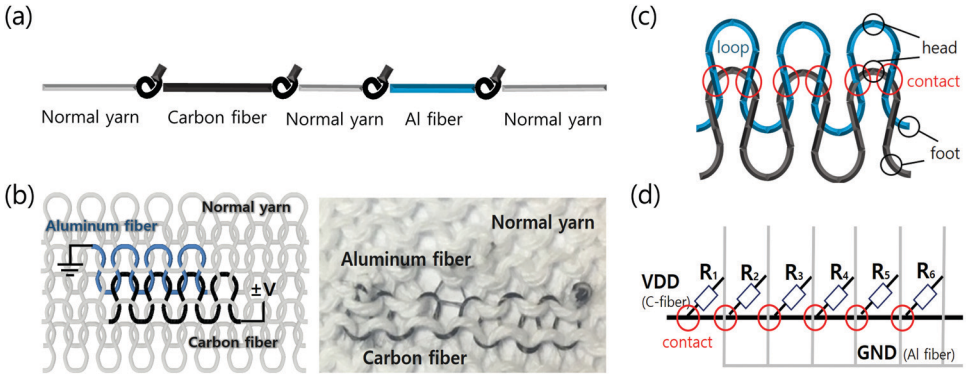

Fig. 2 (a) Yarn consisting of combined carbon fiber, aluminum-coated yarn and cotton yarn that was prepared for the knitted strain sensor, (b) schematic diagram (left) and picture (right) of the knitted-type textile $1 \times n$ array contact using a hand-knitting machine, and (c) schematic structure of the $(1 \times n)$ array RRAM. The blue line represents the aluminum fiber, and the black line represents the carbon fiber. Contact points were created in the area indicated by the red circles, and (d) the $(1 \times n)$ contact array circuit diagram created in the knitted-type sensor.

ratio of 10 and set–reset voltages of within ±3 V. The on/off resistance ratio was maintained stably while device switching was repeated for forty cycles, as shown in Fig. 1c. These characteristics showed that native aluminum oxide on the aluminum surface worked as an insulator layer in the MM structure. This is a benefit of the inherent oxidizing property of aluminum employed in this device, since the resistive switching layer can be achieved without additional deposition steps and conforms to the uneven surface of the yarn.

The knitted-type textile sensor was made with the yarn which had aluminum-coated yarn and carbon fiber yarn inserted in between normal yarn strands as shown in Fig. 2a. Three types of yarn were combined to make one long thread to fabricate the knitted textile. Unlike weaving, which needs two yarn axes, the weft and warp, knitting requires one yarn to interlace the upper row and lower row alternately. Since two different materials, aluminum and carbon, should make contact for a bias applied between them, the cotton yarn between these two yarns supplies insulation. With this specially designed yarn with three materials, we fabricated the textile with resistive switching contacts using a hand-knitting machine, as shown in Fig. 2b. Fig. 2c shows a schematic diagram of where several loops in the basic knitted fabric structure were replaced with carbon fiber and aluminum-coated yarn. The diagram shows that the contact points of the aluminum-coated yarn and carbon fiber yarn were integrated into the fabric structure, which is the MM contact for the strain sensor. Aluminum–carbon contacts are formed between the head and foot of each loop in the knitted structure by controlling the length of different yarns to exhibit a resistance-changing contact for the sensor device. The MM contact array could be used as a series of $(1 \times n)$ arrays of cross-contact devices, as can be seen in Fig. 2d, and also maintained the resistive switching characteristics of a previous study and conventional single RRAM devices. The uniformity of the aluminum particles on the aluminum-coated yarn surface was observed through scanning electron microscopy (SEM) and energy dispersive X-ray spectroscopy (EDS) (data shown elsewhere).[10]

The figure showed that the aluminum-coated yarn and the carbon fiber yarn were interlaced to make a series of contacts and were knitted in the same shape to other parts of the textile. The schematic view of the knitted resistive switching device structure and circuit diagram is illustrated in Fig. 2c. This MM contact array could be used as a $1 \times n$ array of cross-contacts for the resistance-changing device. By varying the length of each section of different yarn, it is possible to control the number of contacts between aluminum and carbon. In this sample, three loops of carbon fiber and aluminum-coated yarn are interlaced to form six contact points, a series of 1×6 devices.

The *I–V* and endurance characteristics of the textile-type RRAMs, a series of six devices as shown in Fig. 2d, along the cyclic tests are shown in Fig. 3. The resistive switching between HRS and LRS is stable, with an on/off resistance ratio of more than 10 and a set–reset voltage of within ±3 V, as shown in Fig. 3a. To establish a standard on/off resistance ratio, the resistance data were collected at the (0.3 V) read voltage after each negative/positive voltage sweep. Also, the endurance characteristics of the switching operation are observed to be stable along the cyclic tests, as shown in Fig. 3b, demonstrating that it can still work as a RRAM when the properties need to be combined.

We carried out current–voltage measurements of knitted devices with stretching either horizontally or vertically, as shown in Fig. 4 and 5, respectively, to prove that the knitted-type RRAM device can be applied to the textile strain sensor. The device was horizontally stretched from 35 mm to 50 mm at intervals of 5 mm and then released to be recovered to 35 mm. The horizontal stretching test was performed by pulling both horizontal ends of the device. Fig. 4a shows the *I–V* curve of the original, stretched, and recovered state with horizontal stretching. It can be seen that the on/off ratio becomes smaller in the stretched state but recovers to the original value in the recovery state. This was the gradual change in resistance along the stretch [Fig. S1, ESI†]. The difference between the length of the original sample (L_o) and the length of the stretched sample (L) were divided by L_o, and this value was defined as the strain (%). And the current and resistance according to the strain (%) were measured. The variation of the resistance of the device in the HRS and the LRS along the strain caused by stretching is shown in Fig. 4(b) with red circles and black squares, respectively. From these measurements, it is

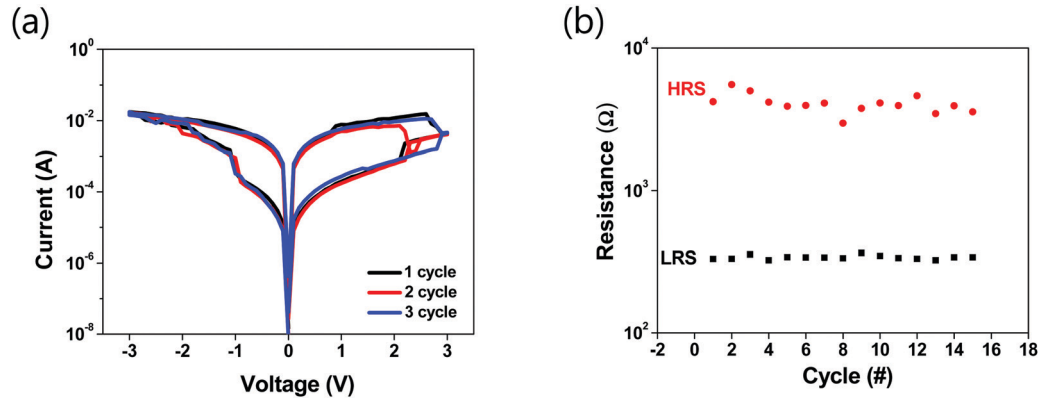

Fig. 3 Knitted RRAM characteristics: (a) *I*–*V* characteristics of the stable set/reset properties, and (b) endurance characteristics of the textile-type RRAM device along the cyclic tests.

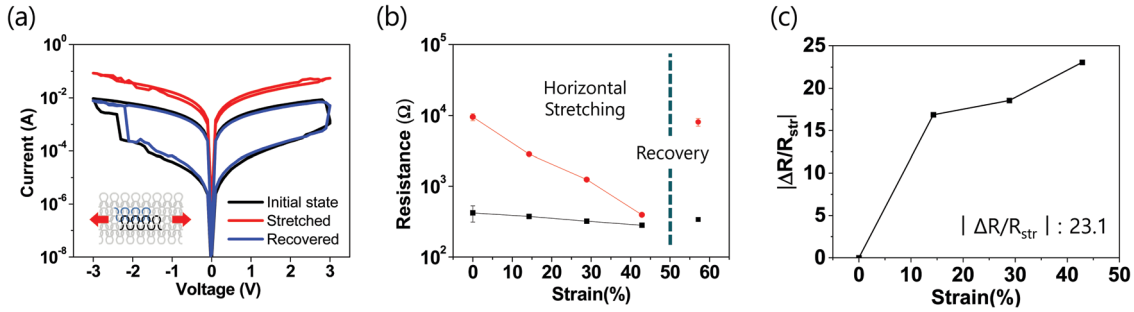

Fig. 4 Knitted RRAM characteristics depending on horizontal stretching: (a) *I*–*V* curve of the original, stretched, and recovered state by horizontal stretching (where the inset shows a schematic of the horizontal stretching test), (b) HRS/LRS resistance depending on a strain generated *via* horizontal stretching (HRS is indicated by the red line and LRS is indicated by the black line), and (c) normalized variation of the resistance ($|\Delta R/R_{str}|$) in HRS depending on a strain generated *via* horizontal stretching.

shown that the larger change in resistance in the HRS rather than the LRS can easily be utilized for the strain sensor. Therefore we normalized the variation of resistance in the HRS between the stretched state and the original state (ΔR) in Fig. 4c through eqn (1). The $|\Delta R/R_{str}|$ value was calculated by dividing the resistance change of the stretched state and the original state (ΔR) in HRS by the resistance value of the stretched state (R_{str}).

$$|\Delta R/R_{str}| = |(R_{HRS,stretched} - R_{HRS,original})/R_{HRS,stretched}| \quad (1)$$

During the stretching process, the difference in resistance values between the HRS and the LRS gradually decreases, and when the device was recovered, the resistance values in both the HRS and LRS were recovered. It is noticeable that the change of $|\Delta R/R_{str}|$ of the knitted sensor in this work is evidently larger than other strain sensors previously reported, and ranged between 0.16 and 3.5, which will be discussed later.

The variation with vertical stretching was also checked. The device was vertically stretched from 35 mm to 50 mm at

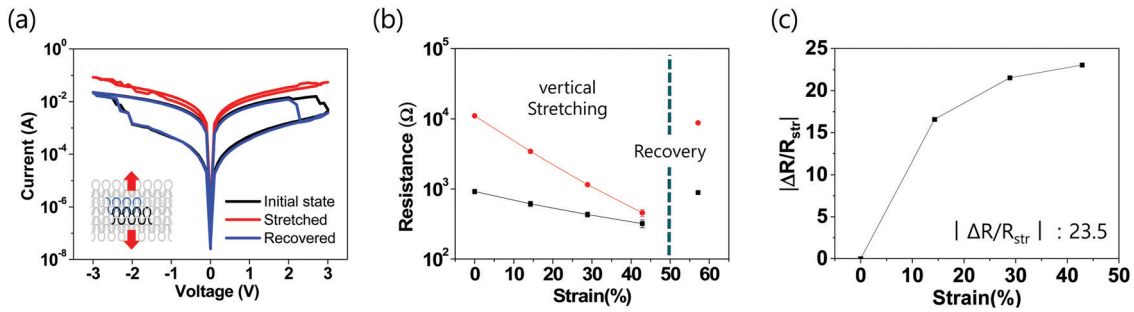

Fig. 5 Textile-type RRAM characteristics depending on vertical stretching: (a) *I*–*V* curve of the original, stretched, and recovered state by vertical stretching (where the inset shows a schematic of the vertical stretching test), (b) HRS/LRS resistance depending on a strain generated *via* vertical stretching (HRS is indicated by the red line and LRS is indicated by the black line), and (c) normalized variation of the resistance ($|\Delta R/R_{str}|$) depending on a strain generated *via* vertical stretching.

intervals of 5 mm, as with earlier horizontal stretching, and then recovered to 35 mm and the *I–V* curve of the original, stretched, and recovered state with vertical stretching is shown in Fig. 5a [Fig. S2, ESI†]. Fig. 5b shows the characteristics of the device along the strain, and the normalized variation of the resistance ($|\Delta R/R_{str}|$) calculated in shown in Fig. 5c. During the vertical stretching process, the resistance tends to gradually decrease, and when the device was recovered the ratio recovered was similar to the horizontal stretching test.

The newly developed sensor, using a resistance value that varies with the number of conductive filaments of the HRS in RRAM switching, has a high $|\Delta R/R_{str}|$ compared with other textile-type strain sensors that use only the change in contact resistance between the two materials. This abrupt resistance change is useful for constructing great stretch-sensitive strain sensors compared with typical wearable strain sensors.[30–32]

When the knitted RRAM is stretched on this fabric, the contact area between aluminum and carbon increases due to deformation of the fabric structure, which causes lowering of the resistance by enlarging the electrical path through contact between the Al and C yarns. This is why we chose the knitted structure over the various other woven structures. For woven structures, the contact between the yarns, for the weft and warp components, is very tight and not stretchable due to the intrinsic structure, and the contact area hardly changes when stretched. On the other hand, the knitted structure allows the total contact area to be changed significantly with stretching. Therefore, the knitted structure was adopted in this study. Fig. 6 shows a schematic diagram demonstrating the change when an interlaced part of the knit structure is stretched and recovered. The contact area between the two yarns is marked in red. As the knitted sensors are stretched, the area where the two yarns overlap with each other to make physical contact is increased. (Fig. 6b). The decrease of the on/off resistance ratio through increasing the aluminum–carbon contact area can be explained by conductive filaments (CFs), which act as conducting paths in the RRAM. The resistance of the RRAM device formed with contact between aluminum and carbon depends on a switching mechanism induced by an oxygen-controlled chemical reaction that repeatedly creates and removes conducting filaments along the bias applied.[23,33] Typical RRAMs have a low resistance because a lot of CFs are formed in the 'on' state (LRS), and have a high resistance because most CFs are ruptured in the 'off' state (HRS). However, as the aluminum–carbon contact area becomes larger along the stretch, the total number of CFs remaining unruptured in the HRS is sufficient to act as a conducting path to increase the current level. In turn, the HRS resistance becomes similar to the resistance of the LRS without the set bias being applied. Also, the number of pinholes in the thin native aluminum oxide layer increases as the aluminum–carbon contact area is enlarged by the stretch, so that the current flow through the dielectric layer increases.[34–36] Since stretching the knitted sensor means an increase in the aluminum–carbon contact area, the resistance of the LRS decreases with the stretching process and the on/off resistance ratio becomes smaller. When discussing the sensitivity of the knitted sensor using this principle, it can be seen that the change of $|\Delta R/R_{str}|$ with stretching can be used to have the same meaning. The relationship between the aluminum–carbon contact area and the change in resistance is checked by varying the contact area on the flat device, as can be seen in Fig. S3 (ESI†).

The gauge factor, defined as $|\Delta R/R_0|$, is a common parameter to demonstrate the sensitivity of sensors. In this work, the resistance value of the stretched state is lower than for the initial state, while the resistance value of the stretched state is higher than the initial state in most conventional strain sensors. Since R_0 is the lowest resistance value in conventional strain sensors, we used the lowest resistance R_{str} to show the sensitivity of the sensors developed in this work. Although direct comparison is difficult because it is not exactly the same parameter as the gauge factor, it can be used for a sensitivity comparison in the sense that it is a value obtained by dividing the resistance change by the minimum resistance value. If the gauge factor, which is a common parameter, is calculated using $|\Delta R/R_0|$, the developed device has a value of '0.9'. This value cannot intuitively show the resistance change of the developed device and, as discussed above, it was judged that it is appropriate to compare the sensitivity through $|\Delta R/R_{str}|$ rather than $|\Delta R/R_0|$. The maximum of the $|\Delta R/R_{min}|$ and the average of $|\Delta R/R_{min}|$ for recently developed textile-type strain sensors[31,32,37,38] are shown in Table 1 and Fig. 7, respectively. $|\Delta R/R_{str}|$ was used for the knitted sensor developed in this work for the comparison since it presents the change in resistance along the strain effectively. Unlike previously reported fabric-type sensors with $|\Delta R/R_{min}|$ values as low as 0.2 to 3.5, newly developed Al–C textile-type strain sensors have been found to have $|\Delta R/R_{min}|$ values of approximately 20 by adjusting the

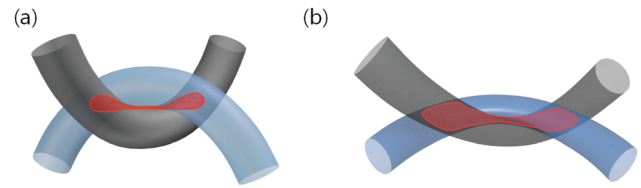

Fig. 6 Schematic diagram showing the change for part of the knitted structure with stretching (the contact area between the two yarns is marked in red): (a) original and recovered knitted structure with the aluminum-coated yarn and the carbon fiber yarn, and (b) stretched knitted structure with the aluminum-coated yarn and the carbon fiber yarn.

Table 1 $|\Delta R/R_{min}|$ values of newly developed and recently reported knitted-type strain sensors.[31,32,37,38] The $|\Delta R/R_{str}|$ value was used instead of $|\Delta R/R_{min}|$ in this comparison because the R_{str} value is the minimum resistance state value in this study

No.	$\lvert\Delta R/R_{min}\rvert$ (max)	Materials used	Fabricated structure	Ref.
This work	23.1	Al, C	Knitting	—
1	2.0	Ag	Knitting	31
2	0.2	PEDOT	Coating on fabric	32
3	3.5	RGO	Coating on fabric	37
4	2.7	PEDOT:PSS	Knitting	38

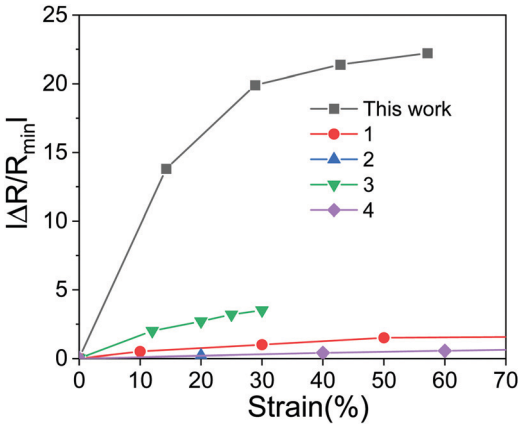

Fig. 7 $|\Delta R/R_{min}|$ maximum values along the strain of newly developed and previously reported knitted-type strain sensors.[31,32,37,38]

number of Al–C contact points. This means that the newly developed device can be used as a very sensitive strain sensor that can detect a significant difference even with a small applied strain, and it is expected that these can be applied to body parts with a small maximum range of motion.

Fig. 8 shows the variation of the resistance during repeated stretching operations with 43% strain over cycles and times. Fig. 8a and b show the variation of the resistance with horizontal and vertical stretching, respectively. Odd numbers of cycles represent the recovery states, and even numbers of cycles represent the stretch states. The change in resistance when the sensor is stretched in the horizontal and vertical directions was also measured over time. (Fig. 8c and d, respectively). In each of these four cases, the resistance ratio in the stretching and recovery states was more than ten and stable. It shows remarkable resistance differences for the stretch states and recovery states as much as applicable for a strain sensor. With these results, we confirmed that the knitted-type RRAM could be applied as a wearable textile strain sensor.

Aluminum-coated yarn and carbon fiber yarn stretching tests were conducted to verify that the on/off resistance ratio change of 10 or more in the textile strain sensor was due to the MM contact area change in the RRAM device and not deformation of the conducting yarn in the knitted structure. The samples for the stretching test were fabricated using either two aluminum-coated yarns or two carbon fiber yarns only, in the same manner as the knitted structure shown in Fig. 2. The current flow through the structural contacts between two unconnected yarns embedded in the knitted structure was measured to observe the change in resistance under stretching. The variation in resistance of the aluminum-coated yarn and the carbon fiber yarn upon horizontal/vertical stretching is shown in Fig. 9. For the aluminum-coated yarn sample, during the horizontal and vertical stretching processes, the resistance was reduced from 13.8 Ω to 7.3 Ω and from 15.5 Ω to 3.7 Ω (Fig. 9a and b). For the

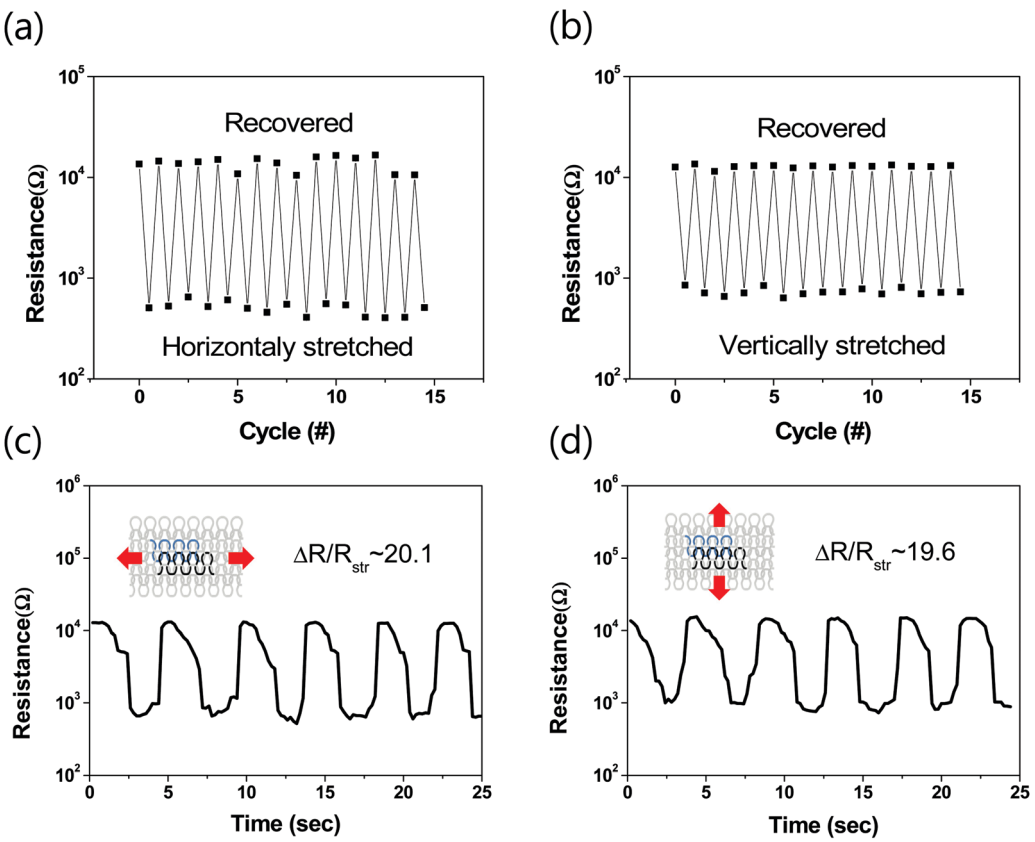

Fig. 8 (a) Resistance variation along repeated horizontal stretching operations; odd numbers are the recovery state, and even numbers are the stretched state, (b) repetition of vertical stretching and recovery slowly over time, and (c and d) the same manner of horizontal and vertical stretching operations.

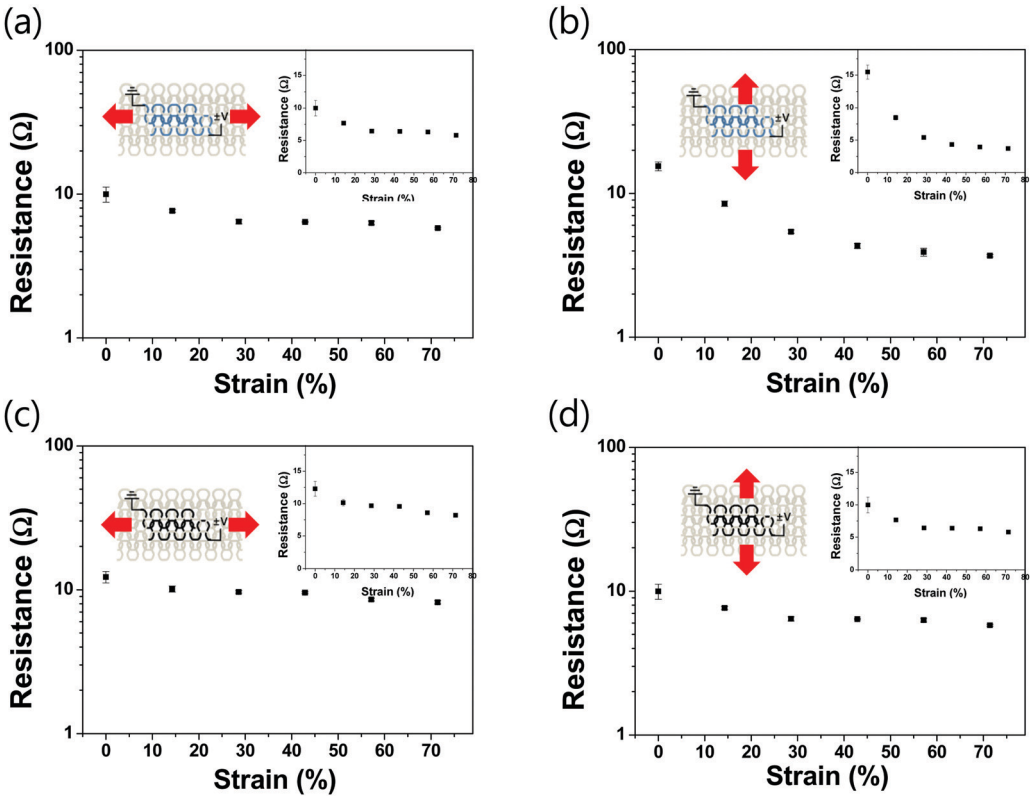

Fig. 9 Resistance variations of single-type conducting yarn structures (aluminum-coated yarns only or carbon fibers only) under stretching: (a) aluminum-coated yarn under horizontal stretching, (b) aluminum-coated yarn under vertical stretching, (c) carbon fiber yarn under horizontal stretching, and (d) carbon fiber yarn under vertical stretching.

carbon fiber yarn sample, during the horizontal and vertical stretching processes, the resistance was reduced from 12.3 Ω to 8.2 Ω and from 10 Ω to 5.8 Ω (Fig. 9c and d). It was demonstrated that the resistance in this sample was only 1.8, 4.1, 1.5, and 1.7 times the difference when only the knitted structure was applied for the strain test, while the HRS resistance in the resistive switching device was slightly different from 10^1 to 10^2 times. The samples shown in Fig. 9 and the fabric strain sensors in other studies are fabricated using one conducting material for the current to flow through the connected yarns or contacts between the same materials to show a resistance change along with the stretching.[31,32,37,38] Existing textile-type strain sensors fabricated with a built-in yarn or a fabric made of one material mainly use changes in the fabric structure and the number of cracks. These strain sensors have a small resistance ratio because there are limits to the resistance change according to variations in the number of cracks and the strain of the entire textile structure. However, the newly developed aluminum–carbon contact strain sensor showed a drastic resistance change ratio of 10 times or more since the current flow is through different materials of the RRAM in the HRS. It is identified that the large changes in resistance and the on/off resistance ratio were due to the MM contact area change in the RRAM, unlike other strain sensors.

To verify the reliability of the textile-type RRAM strain sensor, the stretching test and measurement of the output voltage change were performed simultaneously. A simple voltage divider circuit (Arduino) was applied to measure the voltage output during stretching and recovery of the sample, as shown in Fig. 10a. The circuit is designed to apply a fixed voltage with a resistor while connected to the two electrodes of the sensor and to record the voltage output that changes according to the resistance change of the sensor. The Arduino circuits and devices were connected using special sample-fixing pins in automated machines for measuring electrical properties, and changes in the output voltage due to stretching and recovery were observed over time (Fig. 10b). A 70 mm sample with both ends fixed was set in one cycle to stretch and recover a strain value of 0.5 over 6 seconds. Fig. 10c shows the static reliability of the textile strain sensor after stretching and recovery over 500 cycles. The stretching test method followed the international standardization (IEC 62899-202-4) for stretchable electronics.[39] The resistance was measured 5 times after 1, 100, and 500 cycles to obtain an average value, and it was verified that the on/off resistance ratio was maintained at more than 10 even after 500 cycles.

Considering that the wearable devices should perform on a curved human body, and not just on a flat surface, the sensing characteristics along the stretch due to the movement of the knee joint were evaluated. The knitted-type strain sensor was fabricated in the form of a sleeve with a circumference around the knee and a length of 30 cm, as can be seen in Fig. 11, which

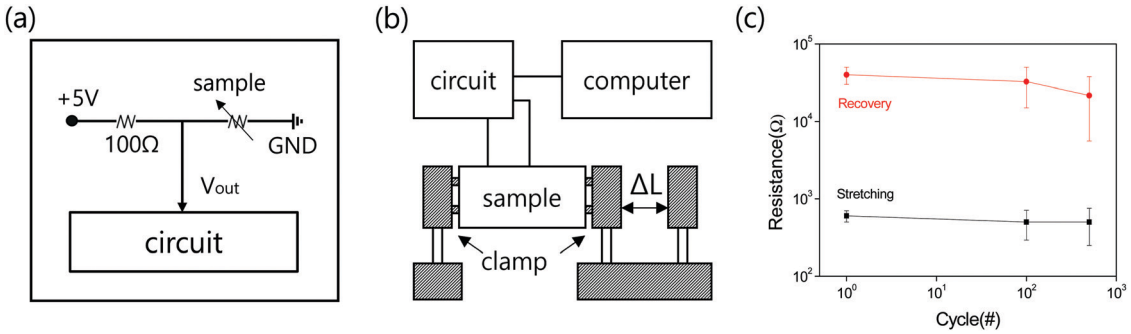

Fig. 10 Reliability measurement for repetitive stretching: (a) voltage divider circuit design for measurement of the variation of resistance during knee flexion and recovery, (b) equipment set up for reliability measurement of the textile-type strain sensor, and (c) static reliability verified by the resistance value measured 5 times over 500 stretching cycles.

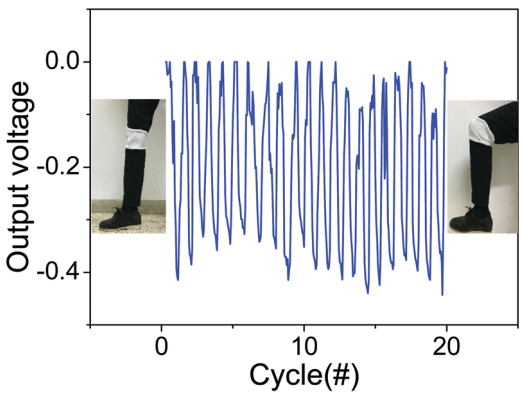

Fig. 11 Application to the knee joint of the knitted RRAM strain sensors integrated with a sleeve. Output voltage variation through the voltage divider connected to the sensors during repeated flexion and recovery.

could be fabricated as a whole garment with built-in strain sensors by further knitting above and below the device. The knitted knee sleeve with integrated RRAM sensors was worn on the joints of the person to check if the sensing performance in a real situation works as already seen in flat stretching measurements previously shown. A voltage divider circuit was used to measure the voltage output during bending and flattening of the knee. The circuits and devices were connected using a long conductive thread to prevent them from being disconnected through movement, which happens in the case of soldered wire connections. As the bending and flattening of the knee occurred over repeated cycles, the variation of voltage output values according to the voltage divider circuit of the strain sensor remained stable. Therefore, it is expected that the fabric-type resistance strain sensor can be built in the same way as conventional clothes without any discomfort.

4. Conclusion

In conclusion, a new knitted type of textile strain sensor that uses resistance-change characteristics, comprising aluminum-coated yarns and carbon fibers, has been developed and its functionality in a repeatable, wearable device was demonstrated. This study is noteworthy since it used a resistance-variation mechanism that depends on the change of the contact area in the knitted-type sensors from a combination of two different materials, and not the resistance change according to the stretching of the single kind of conducting yarn itself, which is the case for general wearable strain sensors reported in other studies. The developed textile strain sensor based on a knitted structure and aluminum–carbon yarns showed a large change in resistance of more than 10 times in the non-stretched (recovery) state and stretched state (with 43% strain) either vertically or horizontally. Through repeated stretching operations, it was confirmed that a stable resistance change was maintained, even after repetitive deformation and recovery cycles. It is suitable for application in wearable sensors in that the change of resistance with deformation is highly sensitive and has a low driving voltage. We expect that these knitted strain sensors can be used for monitoring vigorous motions performed by humans, such as jumping, marching, jogging, bending, and rotation of the joints, indicating their tremendous potential for applications in wearable electronics. This concept can be readily extended to other fabrics, such as cotton, wool, and other fabrics made of artificial or natural fibers. The fabrication method used in this study, which can utilize existing knitting machinery in textile industries, paves the way for a new method of low-cost and large-scale fabrication of wearable sensors, and is expected to present a new vision for the study of other types of textile-type sensors as well as strain sensors.

Author contributions

Junhyeok Jang, Suji Kim, and Mijung Lee: initiated the idea, designed the experiments and analyzed the results through constructive discussions.

Seungjun Park, Kangmin Lee, Geum-young Park, Byoung-Joon Kim, and Junghun Oh: performed and advised on the experiments.

Conflicts of interest

The authors declare that they have no known competing financial interests or personal relationships that could have appeared to influence the work reported in this paper.

Acknowledgements

This work was supported by the National Research Foundation of Korea (NRF) funded by the Korean Government grant (2015R1A5A7037615, and 2019R1A2C1010664) of the Republic of Korea.

References

1 M. Di Rienzo, F. Rizzo, G. Parati, G. Brambilla, M. Ferratini and P. Castiglioni, MagIC system: A new textile-based wearable device for biological signal monitoring. applicability in daily life and clinical setting, *2005 IEEE Engineering in Medicine and Biology 27th Annual Conference*, 2005, pp. 7167–7169, DOI: 10.1109/IEMBS.2005.1616161.

2 M. Chen, Y. Zhang, Y. Li, M. M. Hassan and A. Alamri, AIWAC: Affective interaction through wearable computing and cloud technology, *IEEE Wireless Commun.*, 2015, **22**(1), 20–27.

3 Z. E. Brewer, H. C. Fann, W. D. Ogden, T. A. Burdon and A. Y. Sheikh, Inheriting the learner's view: A google glass-based wearable computing platform for improving surgical trainee performance, *J. Surg. Educ.*, 2016, **73**(4), 682–688.

4 A. M. Hussain, F. A. Ghaffar, S. I. Park, J. A. Rogers, A. Shamim and M. M. Hussain, Metal/polymer based stretchable antenna for constant frequency far-field communication in wearable electronics, *Adv. Funct. Mater.*, 2015, **25**(42), 6565–6575.

5 X. Huang, Y. Liu and K. Chen, *et al.*, Stretchable, wireless sensors and functional substrates for epidermal characterization of sweat, *Small*, 2014, **10**(15), 3083–3090.

6 L. Kou, T. Huang and B. Zheng, *et al.*, Coaxial wet-spun yarn supercapacitors for high-energy density and safe wearable electronics, *Nat. Commun.*, 2014, **5**, 3754.

7 D. Son, J. Lee and S. Qiao, *et al.*, Multifunctional wearable devices for diagnosis and therapy of movement disorders, *Nat. Nanotechnol.*, 2014, **9**(5), 397.

8 J. Han and M. Meyyappan, Copper oxide resistive switching memory for e-textile, *AIP Adv.*, 2011, **1**(3), 032162.

9 S. Yi, I. Choi, B. Kim and Y. Joo, Reliability issues and solutions in flexible electronics under mechanical fatigue, *Electron. Mater. Lett.*, 2018, **14**(4), 387–404.

10 A. Jo, Y. Seo and M. Ko, *et al.*, Textile resistance switching memory for fabric electronics, *Adv. Funct. Mater.*, 2017, **27**(15), 1605593.

11 A. C. Siegel, S. T. Phillips, M. D. Dickey, N. Lu, Z. Suo and G. M. Whitesides, Foldable printed circuit boards on paper substrates, *Adv. Funct. Mater.*, 2010, **20**(1), 28–35.

12 H. M. Lee, S. Choi and K. T. Kim, *et al.*, A novel solution-stamping process for preparation of a highly conductive aluminum thin film, *Adv. Mater.*, 2011, **23**(46), 5524–5528.

13 F. M. Brower, N. E. Matzek and P. F. Reigler, *et al.*, Preparation and properties of aluminum hydride, *J. Am. Chem. Soc.*, 1976, **98**(9), 2450–2453.

14 J. A. Haber and W. E. Buhro, Kinetic instability of nanocrystalline aluminum prepared by chemical synthesis; facile room-temperature grain growth, *J. Am. Chem. Soc.*, 1998, **120**(42), 10847–10855.

15 R. J. Jouet, A. D. Warren, D. M. Rosenberg, V. J. Bellitto, K. Park and M. R. Zachariah, Surface passivation of bare aluminum nanoparticles using perfluoroalkyl carboxylic acids, *Chem. Mater.*, 2005, **17**(11), 2987–2996.

16 D. Frigo, G. Van Eijden, P. Reuvers and C. Smit, Preparation and properties of alane dimethylethylamine, a liquid precursor for MOCVD, *Chem. Mater.*, 1994, **6**(2), 190–195.

17 B. Yu and T. Ha, High dielectric performance of solution-processed aluminum oxide-boron nitride composite films, *Electron. Mater. Lett.*, 2018, **14**(5), 563–568.

18 E. McCafferty and J. Wightman, Determination of the surface isoelectric point of oxide films on metals by contact angle titration, *J. Colloid Interface Sci.*, 1997, **194**(2), 344–355.

19 H. M. Lee, S. Choi, A. Jung and S. H. Ko, Highly conductive aluminum textile and paper for flexible and wearable electronics, *Angew. Chem.*, 2013, **125**(30), 7872–7877.

20 D. S. Jeong, R. Thomas and R. Katiyar, *et al.*, Emerging memories: Resistive switching mechanisms and current status, *Rep. Prog. Phys.*, 2012, **75**(7), 076502.

21 J. Y. Seok, S. J. Song and J. H. Yoon, *et al.*, A review of three-dimensional resistive switching cross-bar array memories from the integration and materials property points of view, *Adv. Funct. Mater.*, 2014, **24**(34), 5316–5339.

22 C. Ye, J. Wu and G. He, *et al.*, Physical mechanism and performance factors of metal oxide based resistive switching memory: A review, *J. Mater. Sci. Technol.*, 2016, **32**(1), 1–11.

23 H. P. Wong, H. Lee and S. Yu, *et al.*, Metal–oxide RRAM, *Proc. IEEE*, 2012, **100**(6), 1951–1970.

24 S. Won, S. Y. Lee, J. Hwang, J. Park and H. Seo, Electric field-triggered metal-insulator transition resistive switching of bilayered multiphasic VO x, *Electron. Mater. Lett.*, 2018, **14**(1), 14–22.

25 J. H. Yoon, K. M. Kim and S. J. Song, *et al.*, Pt/Ta2O5/HfO2−x/ti resistive switching memory competing with multilevel NAND flash, *Adv. Mater.*, 2015, **27**(25), 3811–3816.

26 K. M. Kim, D. S. Jeong and C. S. Hwang, Nanofilamentary resistive switching in binary oxide system; a review on the present status and outlook, *Nanotechnology*, 2011, **22**(25), 254002.

27 R. Waser, R. Dittmann, G. Staikov and K. Szot, Redox-based resistive switching memories–nanoionic mechanisms, prospects, and challenges, *Adv. Mater.*, 2009, **21**(25-26), 2632–2663.

28 M. Ismail, C. Huang and D. Panda, *et al.*, Forming-free bipolar resistive switching in nonstoichiometric ceria films, *Nanoscale Res. Lett.*, 2014, **9**(1), 45.

29 Y. Chen, H. Lee and P. Chen, *et al.*, An ultrathin forming-free $\hbox {HfO} _ {x} $ resistance memory with excellent electrical performance, *IEEE Electron Device Lett.*, 2010, **31**(12), 1473–1475.

30 H. Zhang, Flexible textile-based strain sensor induced by contacts, *Meas. Sci. Technol.*, 2015, **26**(10), 105102.

31 O. Atalay, W. Kennon and M. Husain, Textile-based weft knitted strain sensors: Effect of fabric parameters on sensor properties, *Sensors*, 2013, **13**(8), 11114–11127.

32 J. Eom, R. Jaisutti and H. Lee, *et al.*, Highly sensitive textile strain sensors and wireless user-interface devices using all-polymeric conducting fibers, *ACS Appl. Mater. Interfaces*, 2017, **9**(11), 10190–10197.
33 S. Ki Hong, J. Eun Kim, S. O. Kim and B. Jin Cho, Analysis on switching mechanism of graphene oxide resistive memory device, *J. Appl. Phys.*, 2011, **110**(4), 044506.
34 M. A. Wolak, A. S. Wan, J. S. Shirk, M. Mackey, A. Hiltner and E. Baer, Imaging the effect of dielectric breakdown in a multilayered polymer film, *J. Appl. Polym. Sci.*, 2012, **123**(4), 2548–2557.
35 M. Copel, E. Cartier, E. Gusev, S. Guha, N. Bojarczuk and M. Poppeller, Robustness of ultrathin aluminum oxide dielectrics on si (001), *Appl. Phys. Lett.*, 2001, **78**(18), 2670–2672.
36 B. Oliver, Q. He, X. Tang and J. Nowak, Dielectric breakdown in magnetic tunnel junctions having an ultrathin barrier, *J. Appl. Phys.*, 2002, **91**(7), 4348–4352.
37 G. Cai, M. Yang, Z. Xu, J. Liu, B. Tang and X. Wang, Flexible and wearable strain sensing fabrics, *Chem. Eng. J.*, 2017, **325**, 396–403.
38 S. Seyedin, J. M. Razal, P. C. Innis, A. Jeiranikhameneh, S. Beirne and G. G. Wallace, Knitted strain sensor textiles of highly conductive all-polymeric fibers, *ACS Appl. Mater. Interfaces*, 2015, **7**(38), 21150–21158.
39 Maeda S. Conductive ink - measurement methods for properties of stretchable printed layers (conductive and insulating), *Printed electronics*, 2019; IEC 62899-202-4.